Aerodynamics of an Aspect Ratio 8 Wing at Low Reynolds Numbers

J. F. Marchman III* and A. A. Abtahi†
Virginia Polytechnic Institute and State University, Blacksburg, Virginia

Wind tunnel tests were conducted on an aspect ratio 8, Wortmann FX-63-137, untapered, unswept wing at chord-based Reynolds numbers of 70,000-300,000. Lift, drag, and pitching moment data were obtained in a wind tunnel with freestream turbulence levels of 0.02%. The aerodynamic behavior of the wing is examined through plots of the force and moment data and through flow visualization techniques. The effects of Reynolds number on the traditional aerodynamic behavior as well as on the stall hysteresis loop are examined. The results indicate a strong Reynolds number influence on stall and the resulting hysteresis loop and also a departure to flat-plate aerodynamic behavior at the lowest Reynolds numbers. Flow visualization reveals essentially two-dimensional flow behavior except in the vicinity of the wing tips.

Nomenclature

C = wing chord
C_D = drag coefficient, $= D/\frac{1}{2}\rho V^2 S$
C_L = lift coefficient, $= L/\frac{1}{2}\rho V^2 S$
C_m = pitching moment coefficient, $= M/\frac{1}{2}\rho V^2 Sc$
D = drag
L = lift
M = pitching moment (taken $C/4$)
Re_c = Reynolds number based on chord, $= \rho Vc/\mu$
S = wing planform area
V = freestream velocity
α = wing angle of attack
μ = freestream flow viscosity
ρ = flow density

Introduction

MOST past research on airfoil aerodynamics has concentrated on chord Reynolds numbers above 500,000, since few aircraft have operated below that value. Recently, however, there has been increased interest in the behavior of airfoils and wings operating at Reynolds numbers below 500,000. Few aircraft other than model airplanes have flown in this lower range of Reynolds numbers in the past; however, current interest in the development of low-speed remotely piloted vehicles (RPVs) and in high-altitude stationkeeping aircraft has prompted a new interest in this flight regime.

Low Reynolds number flight is usually thought of as very-low-speed flight or flight using a wing with small chord length; however, examining the definitions of Reynolds number and lift coefficient

$$Re = \frac{\rho Vc}{\mu} \qquad L = C_L S \frac{\rho}{2} V^2$$

it can be seen that Reynolds can be defined in terms of wing loading (L/S) and C_L to give

$$Re_c = \frac{2c}{\mu V} \frac{1}{C_L} \frac{L}{S}$$

Therefore, an aircraft of low wing loading operating at high lift coefficients may find itself in a low range of Reynolds number.

Most data obtained in the past for wings at low Reynolds numbers have come from model airplane or sailplane enthusiasts. The earliest such work was that of Schmitz[1] for model airplane wings. Schmitz was the first to report the now fairly well-known stall hysteresis effect seen on airfoils at low Reynolds numbers. In another effort to provide data to model airplane designers, Althaus[2] of the University of Stuttgart studied a selection of airfoils and obtained two-dimensional lift and drag data. Other studies were conducted at the University of Delft,[3] again determining only lift and drag for two-dimensional airfoil sections.

In 1981, as interest in low Reynolds number airfoil performance increased in the United States, Carmichael[4] published an excellent survey paper on the subject. Within the last few years, interest has continued to increase and research is now being performed in several U.S. universities. Most of this work, however, still appears to concentrate on two-dimensional airfoils rather than three-dimensional wings and to examine only lift and drag behavior. No pitching moment data have been published at this time.

Low Reynolds number wing aerodynamic research is difficult and requires special facilities. Wind tunnels used for such research must have very low turbulence levels in their flows and be acoustically quiet since ambient turbulence and noise can artifically trip the boundary layer, thus masking the true low Reynolds number behavior. Measurement of the forces on a wing at low Reynolds numbers may be quite difficult due to the low forces involved and to the possibility of improperly installed surface pressure taps tripping the boundary layer. Remote control of the test model is essential if the researcher is to have any hope of detecting the low Reynolds number stall hysteresis loop. Thus, due to poor wind tunnel flow quality and the lack of sensitive force balances and model control equipment, low Reynolds number airfoils or wing research cannot be conducted at most research facilities.

The Virginia Tech Stability Wind Tunnel is one of the few facilities capable of this type of research, having documented freestream turbulence levels of about 0.02% and excellent remotely operated strain gage balance equipment. The turbulence level in the Stability Wind Tunnel has been extensively documented by Saric[5,6] and was verified repeatedly by use of hot-wire surveys of the test section during the reported tests.

The present study was conducted in this facility in an attempt to obtain full three-dimensional aerodynamic data on a

Received Dec. 4, 1984; presented as Paper 85-0278 at the AIAA 23rd Aerospace Sciences Meeting, Reno, Nev., Jan. 14-17, 1985; revision received March 18, 1985.

*Associate Professor of Aerospace and Ocean Engineering. Associate Fellow AIAA.
†Graduate Research Assistant.

wing of aspect ratio 8 at Reynolds numbers below 500,000. This study was conducted as a preliminary study leading to research on aspect ratio effects in low Reynolds number aerodynamics. Data were obtained using a specially modified six-component strain gage balance system as well as by use of the momentum deficit method and from integrated chordwise pressure distributions.

The strain gage balance used in these tests was designed and built by NASA Langley Research Center for use in the Stability Wind Tunnel and is designed to be accurate at low speeds. As will be discussed later, the accuracy of the gage was verified by the repeatability of the results. The only exception was at the lowest Reynolds number tested (70,000) where results contained unacceptable scatter. Since other researchers have questioned the accuracy of strain gage balances in low Reynolds number tests, comparisons were made with other test methods and will be discussed later.

Experimental Technique

Low Reynolds number testing is very sensitive to ambient wind tunnel turbulence levels and to tunnel acoustics. Considerable uncertainty exists about the accuracy of some previous low Reynolds number research because of the relatively high levels of ambient turbulence in the test facilities used. The present tests were conducted in the Virginia Tech Stability Wind Tunnel, a closed-circuit facility with a $6\times6\times28$ ft test section. This tunnel has an unusually low-turbulence level for a tunnel its size because of its seven sets of antiturbulence screens upstream of the test section and because of a large air exchange tower, which appears to be quite effective in isolating the test section from any fan acoustic and pressure pulse effects.[5,6] During the tests, freestream turbulence levels were repeatedly measured at 0.02% at the model location for a model Reynolds number of 150,000. Previous studies performed in this wind tunnel, during which extra freestream turbulence was deliberately introduced, showed that the added turbulence can reduce or eliminate the stall hysteresis effect. Hence, it is extremely important that low Reynolds number aerodynamic research be conducted only in facilities with very low ambient turbulence levels.

The model used for this study was made with the contour of a FX-63-137-ESM airfoil. The FX-63-137 airfoil was developed by F. X. Wortmann of the University of Stuttgart to operate at the comparatively low Reynolds number of 500,000, a typical value for light glider aircraft. Later, when more exact methods of model production were used, it became evident that at the leading edge of this airfoil there was a "flat" area. Eppler of the University of Stuttgart then redefined the coordinates of the airfoil to remedy this situation and designated the modified shape with the letters ESM. Figure 1 shows the contour of the FX-63-137-ESM airfoil.

The chord for the model was chosen to be 5 in. This dictated a span of 40 in. for an aspect ratio of 8. Since the wind tunnel has a width of 72 in., there was ample room on both sides of the wing for wing tip vortices to develop naturally, without any significant wall influence.

The wing itself was machined from a solid block of aluminum in order to meet the tolerances necessary with a model of this size. It was constructed in several pieces to make it possible at a later time to change the aspect ratios. The wing surface was painted dark red in order to enhance flow visualization results.

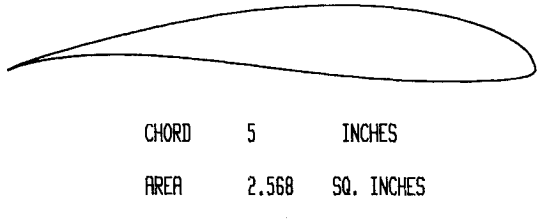

Fig. 1 Wortmann FX-63-137-ESM airfoil.

The model was mounted horizontally on a mechanism that allowed the angle of attack to be changed from outside the test section during operation of the tunnel. Remote operation of angle of attack is necessary if the upper portion of the stall hysteresis loop is to be observed. The reason for this will be discussed when the test data are discussed.

Since the wing model chord was small, the possibility of strut interference had to be considered. Anv interference between the strut and the model would most likely appear as a shift in the zero lift angle of attack. To evaluate the influence of the strut on the test results, tests were run using an inverted model and using an image strut. Tests were also run using a simple flat-plate model of the same planform as the test model. These tests showed that the strut did cause a slight upwash on the wing and all resulting data were corrected to account for this effect.

A special motor-driven, computer-controlled mount was designed and built that fit over the tunnel's six-component strut balance head. The balance then remained stationary, while the model was rotated about the balance in pitch. The entire balance and model mount assembly was shrouded to eliminate strut drag. The balance assembly is shown in Fig. 2.

The output from the strain gage balance was entered into a Hewlett-Packard high-precision, digital voltmeter through a scanner and from there could be read along with all pertinent tunnel data by the Hewlett-Packard 9836 computer currently in use at this facility. This computer also had the capability to remotely control the angle of attack of the model, greatly simplifying the task of conducting the experiments. Figure 3 shows a schematic diagram of the setup used for data acquisition and automatic experiment execution. Each data point taken was actually the average of up to 50 scans by the data acquisition system over a fraction of a second. Scan rates of up to 2000 samples/s were used. Data taken in all but the lowest Reynolds number cases were quite repeatable on successive tunnel entries.

The setup used for the drag measurements by the momentum deficit method was similar in that the computer automatically adjusted the angle of attack of the model and integrated the momentum loss. This momentum loss was measured by obtaining the dynamic pressure loss behind the model, which, in turn, was read into the computer through an electronic manometer and the analog-to-digital converter. The pitot-static tube that obtained the dynamic pressure was continuously swept through the wake of the wing at a constant rate of speed. The computer could then determine the current position of the probe from its initial position and the elapsed time. In order to ensure that no error was being made due to instrument lag, several experiments were conducted using discrete sampling of the wake dynamic pressures. It became evident, however, that there was no noticeable difference between the results of the two methods of sampling. The continuous sampling method proved to be more accurate and faster than the older "wake rake" method.

Flow Visualization Techniques

To gain additional knowledge of the flow phenomena occurring on the wing, flow visualization tests were conducted. The difficulty in using most methods of flow visualization lies in the fact that the technique itself may be intrusive, i.e., may disturb the flow. Tuft methods obviously disturb the boundary layer and will cause transition in a laminar flow. Oil film techniques may also be intrusive with wave formation in the oil film altering local pressures and creating surface ripples.

In order to minimize the possibility of flow intrusion by the flow visualization method, the well-known naphthalene/trichloroethane evaporative film technique was used. This was later supplemented by an oil droplet method.

The naphthalene/trichloroethane evaporative technique uses a small amount of naphthalene dissolved in a trichloroethane solvent and then sprayed on the surface of the wing. Before the evaporation of the trichloroethane solvent, the wing surface (painted red) appears dark under the transparent film. Evaporation of the solvent leaves a thin white coat of crystalized naphthalene, which will itself later evaporate. Properly applied, this method leaves a very smooth, thin white coating on the wing surface that should not alter the behavior of the boundary layer. The technique in these tests had been used previously at Virginia Tech by Saric[5,6] in studies of boundary-layer stability on a flat plate and had been shown to be effective and nonintrusive for boundary-layer flow visualization.

With this technique, the rate at which the color of the wing changes is a function of the mass transfer rate at the surface of the wing. However, this mass transfer rate in itself is quite similar to the wall shear stress. Therefore, it can be said that, in a laminar boundary layer, the evaporation rate is much lower than in a turbulent boundary layer. In this method, a white region usully indicates a region where the flow is laminar. Any dark region must either be a region where there is extremely low mass transfer (as in a separated region) such that the trichloroethane does not evaporate or a region of turbulent flow where the mass transfer is high enough to rapidly sublimate the naphthalene. Naturally, at the separation point, the shear stress vanishes and the mass transfer rate should reach a minimum.

This method gives some valuable information as far as the state of the boundary layer is concerned, but gives no indication of the direction in which the flow is moving. Therefore, it is not possible to demonstrate conclusively the existence of a laminar separation bubble using this method alone.

The method used to determine direction of the surface flow was that of placing small droplets of oil on the surface of the wing and then observing their motion due to the flow. Here it is possible to observe the direction of the flow; however, the small oil droplets create small "bumps" in the surface of the wing and these small bumps disturb the flow. After some experiments, it was ascertained that the droplets must be arranged such that each one does not lie within a 5 deg wedge behind the one ahead if the flow over a droplet is not to be influenced by the wake from an upstream droplet.

Data Analysis

Force balance data were gathered for the model at Reynolds numbers of 70,000-300,000. Obtaining meaningful drag data at Reynolds numbers below 70,000 became increasingly difficult due to the fact that the forces to be measured are extremely low. However, the lift data were very reliable and repeatable over the entire range of test Reynolds numbers. At a Reynolds number of 70,000, the drag data became somewhat unreliable since the minimum drag force at this speed was of the order of only 0.03 lb. On the other hand, at $Re = 300{,}000$, forces can become quite large and, under some conditions, a lift force of nearly 70 lb was generated. This large difference in the order of the forces to be measured is one reason for the difficulty of obtaining good experimental results at low Reynolds numbers.

The authors have confidence in the accuracy of the strain gage data obtained for lift, drag, and pitching moment for Reynolds numbers as low as 100,000. Below that Reynolds number, the drag data become somewhat scattered and, while a general curve that was invariant for successive tests could be fitted through the data, there was significant scatter around the curve. A Reynolds number below 100,000 represents a speed of less than 15 ft/s for a 1 ft chord at sea level. Since it is doubtful that speeds in this range will be encountered even by slow-flying RPVs and since at Reynolds numbers below about 75,000 wing behavior changes to that of a flat plate,[4] no attempts were made to gain improved accuracy at these Reynolds numbers. Again, data taken for Reynolds numbers of 100,000 or more were very repeatable in drag as well as lift and pitching moment.

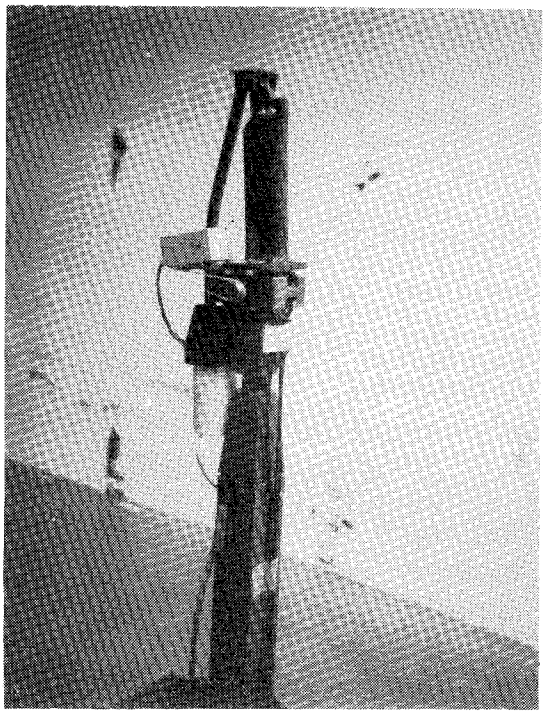

Fig. 2 Strut balance assembly.

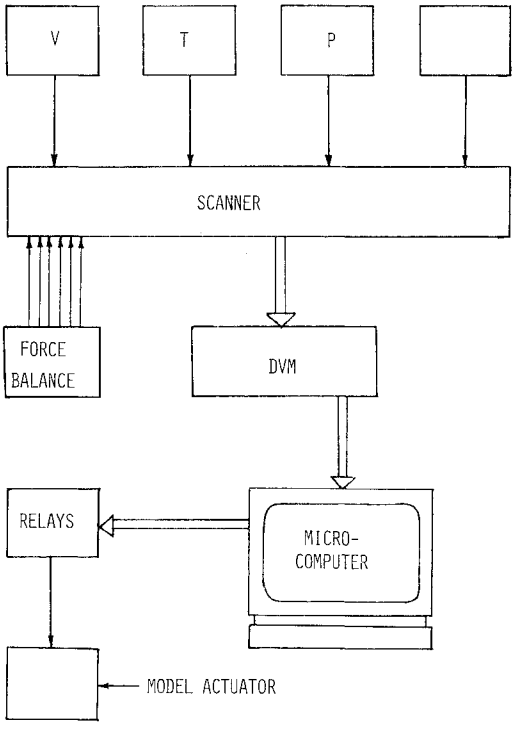

Fig. 3 Model control and data acquisition system.

Figure 4 presents a plot of lift coefficient vs angle of attack for a Reynolds number 200,000. The hysteresis loop is clearly visible in this case. At an angle of attack of about 18 deg $C_{L\max}$ is reached, followed by a decrease in lift coefficient and then a sudden drop at about 23 deg. The shape of the curve indicates a normal stall where separation is moving forward from the trailing edge until a sudden bursting of the laminar separation bubble at the leading edge leads to total upper surface flow separation.

A sequence of flow visualization pictures (Fig. 5) can give some insight into the events taking place as the angle of attack is increased through the point of sharp lift decrease. At low angles of attack, one can see the line of transition at 75% chord. As the angle is increased, the transition line moves steadily forward and a laminar separation bubble appears. This bubble appears as the white area in the lower photo. Transition to turbulent flow causes the bubble to reattach as a turbulent boundary layer. In the literature, this type of bubble is often referred to as a "short bubble." In Fig. 6, one can see an oil flow pattern for an angle of attack where the bubble exists. The oil is pushed forward on a small part of the surface of the wing, indicating a region of separation and backflow. Behind this region the oil is pushed backward again, which means that the flow has become reattached. Figure 5 shows that in this reattached region the naphthalene has already evaporated completely, indicating turbulent flow with corresponding high wall shear stresses and mass transfer rates.

Space limitations preclude a more complete presentation of the flow visualization results; however, the patterns revealed can be summarized for comparison with the figures showing force and moment data. At moderate angles of attack, the wing upper surface experiences laminar flow near the leading edge, followed by laminar separation where adverse pressure gradients are encountered. The free laminar shear layer rapidly becomes turbulent, forcing flow reattachment and a turbulent boundary layer over the remainder of the chord.

As angle of attack is increased, the laminar bubble moves forward and separation of the turbulent boundary layer begins near the rear of the wing. At an angle of attack of about 20 deg, the laminar bubble experiences an adverse pressure gradient sufficient to prevent turbulent reattachment and the entire upper surface flow separates at the point of initial laminar separation.

One objective of this research was to examine the nature of the three-dimensional flow on the wing. Some past research has indicated the possibility of significant spanwise flow with a cellular type of separation. Again referring to the flow visualization figures, it is seen that, except very near the wing tips, the flow behavior is essentially two-dimensional at all angles of attack. Flow near the tips does not appear to differ markedly from that often seen at higher Reynolds numbers.

Figure 4 shows that, at a Reynolds number of 200,000, the stall hysteresis loop exists between about 11 and 23 deg angle of attack. If the wing angle of attack is increased through stall, full stall will occur at approximately 23 deg angle of attack. If the angle of attack is then decreased, the lift coefficient will not retrace the horizontal curve (upper portion of the loop), but will follow the lower part of the loop with full upper surface reattachment not occurring until the angle of attack has been reduced to 11 deg. The laminar separation bubble cannot reform until the pressure gradient over the bubble is sufficiently low, allowing turbulent transition over the bubble to again force turbulent reattachment.

Figure 7 shows the lift data for Reynolds numbers of 70,000, 100,000, and 300,000, in addition to the 200,000 case already shown. Looking first at the 70,000 *Re* case it is seen that the lift curve slope is less than the other cases up to an angle of attack of about 6 deg and then diverges even further. There appears to be a flat-plate type stall at about 6 deg. This is consistent with the behavior reported for other wings at Reynolds numbers below about 75,000 in Ref. 4. For all wings there appears to be some critical value of Reynolds number between about 70,000 and 100,000 where the lift curve behavior changes to that of a flat plate with leading-edge separation at very low angles of attack and no conventional stall or stall hysteresis. Studies are underway at Virginia Tech to determine the influence of aspect ratio on this critical Reynolds number.

At all higher Reynolds numbers, the lift curves are virtually identical until upper surface stall, indicating no *Re* effects on the linear portion of the lift curve in this range and showing again the repeatability of the data and the accuracy of the strain gage measurement technique. It is seen that the hysteresis loop moves to the right as Reynolds number in-

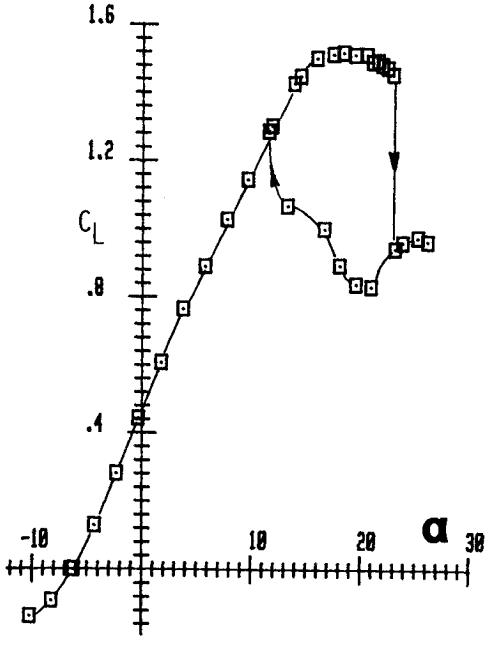

Fig. 4 Lift coefficient data at $Re = 200{,}000$.

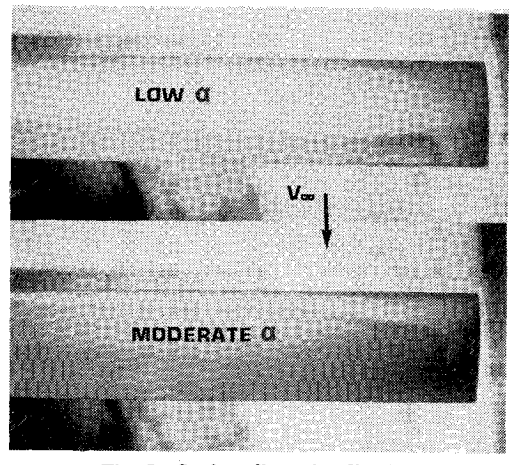

Fig. 5 Surface flow visualization.

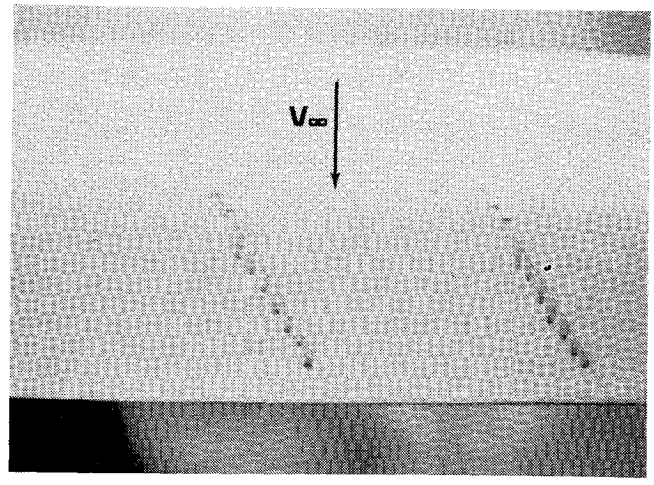

Fig. 6 Oil drop surface flow pattern.

creases, with both the angle of attack where the sudden C_L drop occurs and that where the loop returns to the original curve increasing with Reynolds number.

It is interesting to note that the bottom or return portion of the hysteresis loops at all Reynolds numbers appears to approach the 70,000 Reynolds number curve at the same angles of attack. Essentially, this portion of the hysteresis loop exhibits the same type of flow as the 70,000 *Re* case, with totally separated flow over the upper surface.

It is also seen in Fig. 7 that the zero lift angle of attack is about -6 deg. Previous two-dimensional data[2,7] for this airfoil have shown a zero lift angle of attack anywhere from -5 to -8 deg. This was of some concern to the authors and was examined in some detail. It should be noted that the lift magnitudes found generally agree with those of Ref. 2.

The possibility of strut interference with the flow resulting in a shift of zero lift angle of attack was examined as described previously and the data were corrected to account for this shift. Confidence in the accuracy of the strut angle-of-attack system was high, since it was calibrated before each series of tests and because of the exceptional accuracy of the Schaevitz Engineering LSVP-30 electronic inclinometer that was incorporated into the system.

A study of the literature shows that different values for the zero lift angle of attack have been obtained at different facilities. Reference 7 presents data for a Wortmann FX-63-137 airfoil at a Reynolds number of 280,000. The data in this reference were obtained at the IAG Stuttgart No. 1 wind tunnel. A two-dimensional model with smooth surface was used and the zero lift angle of attack is -8 deg. Other tests run at Virginia Tech[8] have shown that as aspect ratio is increased, α_{L0} increases slightly.

It is interesting to note that tests in a second tunnel (Stuttgart No. 2) with the same model gave a zero lift angle of attack of -6 deg for $Re = 200{,}000$.[7] One must assume that the Stuttgart researchers were equally careful in both investigations and that, since the same model was used in both cases, it is possible for careful research to produce somewhat ambiguous results for α_{L0} at low Reynolds numbers.

In general, tests of small models in large wind tunnel test sections will produce more reliable zero lift angle-of-attack results than those done using larger models in a small tunnel. The reported test results were for a 5 in. chord model tested in a 6×6 ft test section and can be expected to exhibit much less need for correction of data than the results from some previously reported research where wings of twice that chord were tested in tunnels with about one-tenth the test section area. Some previously reported results have included high angle-of-attack data where blockage exceeded the normally accepted limit of 10%. Even with corrections, data taken using large model to tunnel area ratios cannot be accepted without questions about reliability.

The drag data obtained are essentially a reflection of the same phenomena that were described in the previous section. Figure 8 shows a plot of the coefficient of drag vs angle of attack for the two Reynolds numbers of 70,000 and 200,000. Due to the difficulties described earlier, there is a significant spread in the drag data for 70,000. One can, however, still observe the basic nature of the drag curve at this speed. The drag has a minimum at approximately 2 deg. On both sides of this point, it increases as expected and there is no evidence of

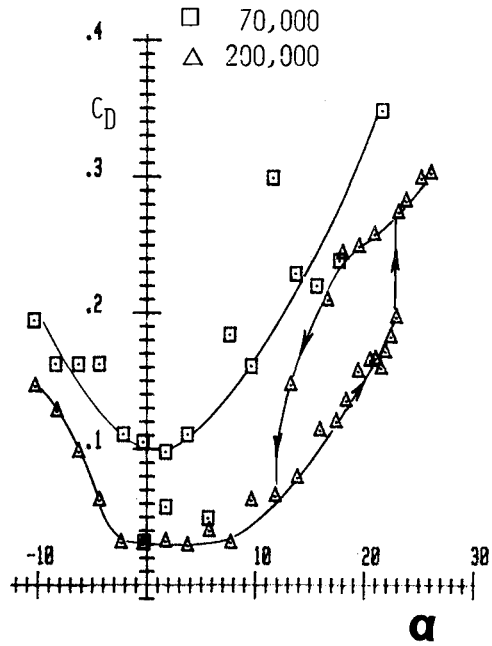

Fig. 8 Drag coefficient behavior at 70,000 and 200,000 Reynolds number.

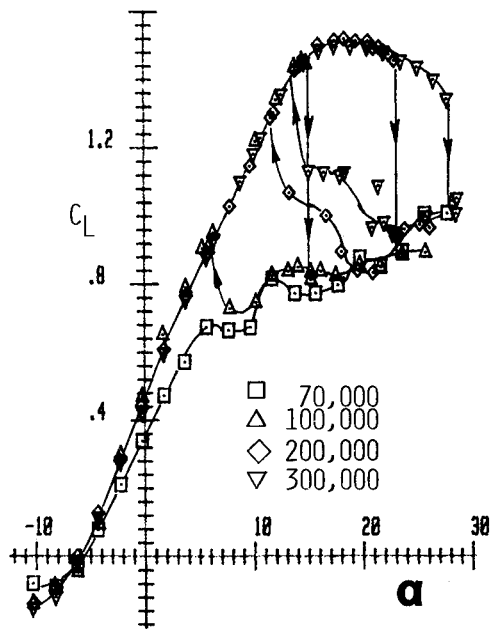

Fig. 7 Lift coefficient data for all *Re*.

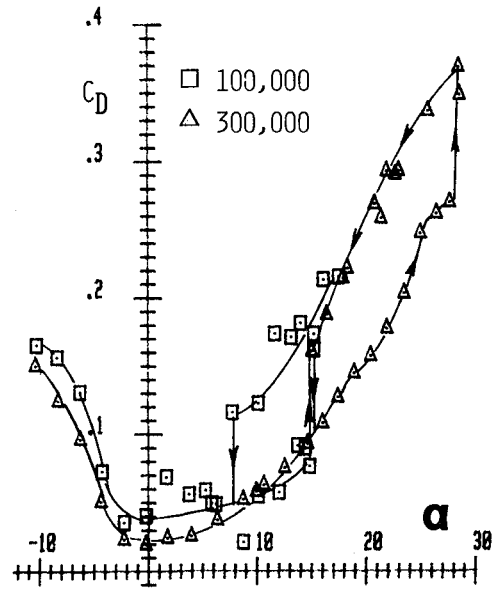

Fig. 9 C_D for $Re = 100{,}000$ and 300,000.

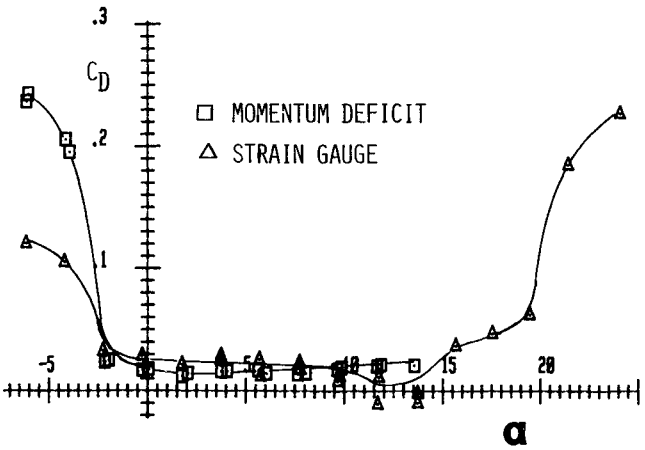

Fig. 10 Comparison of drag measurement technique.

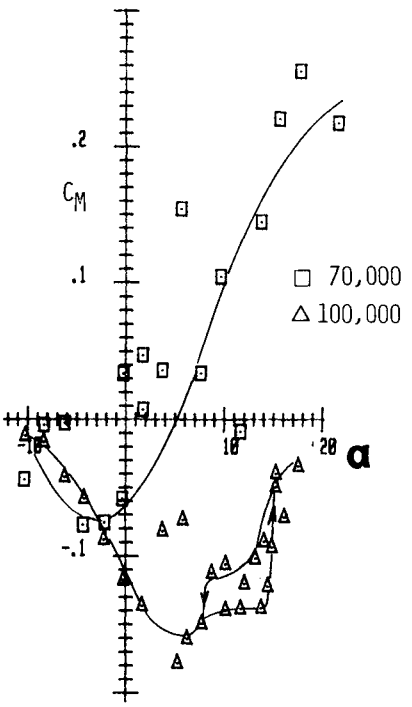

Fig. 11 Moment data at 70,000 and 100,000 *Re*.

hysteresis. At a Reynolds number of 200,000, drag values are significantly lower but the behavior is essentially equivalent. The hysteresis loop that was previously described in conjunction with the lift data becomes visible. The drag values corresponding to the higher lift value on the hysteresis loop are lower than those corresponding to the lower lift values on the loop. The direction in which the wing goes through the hysteresis loop appears reversed from those of the C_L plots since, when the flow separates from the upper surface of the wing, a large wake is generated behind the wing. Drag values remain high until the flow reattaches. The overall decrease of drag in the 200,000 case as compared to the 70,000 case can be attributed to the fact that at the lower Reynolds number the flow is separated at the leading edge for almost the entire range of angles of attack.

Figure 9 shows the drag coefficient behavior for the 100,000 and 300,000 Reynolds number cases. The trends are similar to those shown in Fig. 8 for the 200,000 Reynolds number case. The hysteresis loop has shifted strongly to the right as Reynolds number increased.

Some past researchers have questioned the use of force balances for drag measurement at low Reynolds number

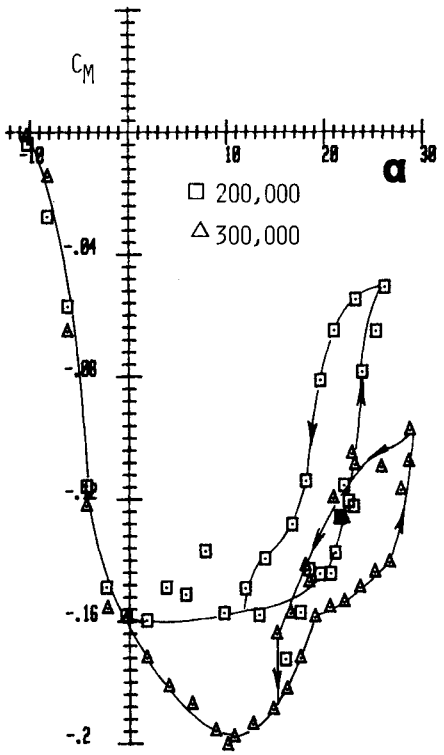

Fig. 12 Moment data at 200,000 and 300,000 *Re*.

because of the low values of drag to be measured. As discussed earlier, the drag values measured by the force balance in these tests were quite repeatable and appeared accurate at all Reynolds numbers above 100,000. Considerable scatter is seen in the 70,000 *Re* data; however, since at this Reynolds number the behavior of the airfoil is that of a flat plate, it is not really in the primary range of interest. Since many past researchers have relied on drag data from momentum deficit measurements, a method that is also somewhat suspect since it is a two-dimensional technique which accounts only for linear momentum losses, some comparisons were made with that method. Figure 10 compares the drag data obtained using the momentum deficit method and the force balance at a Reynolds number of 200,000. The force balance measurements are corrected to infinite aspect ratio by subtracting an induced drag calculated using a computed efficiency factor of 0.85 as obtained from a standard vortex sheet solution for the $\mathcal{R}$ 8 Wortmann wing. Agreement is seen to be fairly good, although obviously it is not perfect.

Other comparisons of drag measurement techniques were made using integrated chordwise pressure distributions (another two-dimensional technique) and were found in even better agreement with the force data than the momentum deficit technique. These are reported in Ref. 8.

Pitching moment data show similar trends to those seen for lift and drag (Figs. 11 and 12). The $Re = 70{,}000$ case displays unstable behavior due to the flow separation on the upper surface of the wing. All of the other cases show at least regions of stable behavior. It should be noted that, at the higher angles of attack, the pitching moment shows the same hysteresis loop as seen before. When the flow is still attached to the surface, the wing shows a stronger tendency to pitch up. This is due to the region of low pressure near leading edge. When the laminar separation bubble bursts and the flow separates, the extent of the low-pressure region around the leading edge drops quickly and the pressure in this region rises, causing an increase in the pitching moment.

Conclusions

In this study, a complete set of data for a wing with an aspect ratio of 8 and a FX-63-137-ESM airfoil section was ob-

tained for Reynolds numbers of 70,000-300,000. This collection of data may be useful for the designer of any aircraft operating at these Reynolds numbers, especially since it includes pitching moment measurements.

The presence of a hysteresis loop in stall was demonstrated. This has far reaching implications for the operation of lifting surfaces at low Reynolds numbers, since it can possibly inhibit stall recovery. Thus, it becomes necessary to take precautions during design that make it highly unlikely that the wings will stall or some provision has to be made for speedy stall recovery. Since at stall the pitching moment increases, as does the drag, while the lift drops much more suddenly, during a normal trailing edge stall the aircraft might become uncontrollable so suddenly that it would be difficult to react fast enough to correct the situation and an automated control device would have to be used.

Comparison of the zero lift angle of attack values found in this study with those in Refs. 2 and 7 indicates some disagreement among zero lift angles of attack found for the Wortmann airfoil. This reinforces the need for testing of wings at low Reynolds numbers in wind tunnels that are large enough to rule out significant blockage effects and that have sufficiently low turbulence levels to reduce the freestream turbulence effects on data.

Previously it had been speculated that the presence of the laminar separation bubble might cause large regions of three-dimensional flow or even three-dimensional separation cells on finite wings. The results of this study indicate that three-dimensional effects do not significantly alter the two-dimensional nature of the flow over the wing and that the effects of the tips are confined to a relatively small region. The effects of the three-dimensional flow around the wing tips appear similar to those observed at much higher Reynolds numbers.

In the future, it will be necessary to collect more data on different airfoil shapes to better understand the influence of different contours on low Reynolds number behavior. More detailed studies of the flow pattern in the laminar separation bubble and of the conditions for reattachment or "bursting" are needed. Even though the airfoil used in this work showed quite good performance, once a deeper understanding of the processes involved is gained, it will be possible to arrive at more efficient shapes that allow vehicles of higher performance to be designed.

Acknowledgment

The research on aspect ratios reported in this paper was sponsored by the Office of Naval Research under Grant N00014-84-K-0093.

References

[1]Schmitz, F. W., "Aerodynamics of the Model Airplane," Ludwig Prandtl Prize for 1941, Translation by Redstone Scientific Information Center, Ala., 1941.

[2]Althaus, D., *Profilpolaren für den Modellflug,* N. V. Neckar Verlag, Villingen-Schwenningen, Univ. of Stuttgart, 1980.

[3]Volkers, D. F., "Preliminary Results of Wind Tunnel Measurements on Some Airfoil Sections at Reynolds Numbers Between 0.6×10^5 and 5.0×10^5," Delft University of Technology, the Netherlands, Memo M-276, June 1979.

[4]Carmichael, B. H., "Low Reynolds Number Airfoil Survey," NASA CR 165803, Nov. 1981.

[5]Saric, W. S. and Yates, L. G., "Generation of Crossflow Vortices in a Three Dimensional Flat Plate Flow," *Proceedings of the Second IUTAM Symposium on Laminar Turbulent*, Novosibirsk, USSR, July 1984.

[6]Reynolds, G. A. and Saric, W. S., "Experiments on the Stability of the Flat Plate Boundary Layer with Suction," AIAA Paper 82-1026, June 1982.

[7]Miley, S. J., "A Catalog of Low Reynolds Number Airfoil Data for Wind Turbo Applications," Dept. of Aerospace Engineering, Texas A&M University, College Station, Feb. 1982.

[8]Marchman, J. F. III, Abtahi, A. A., and Sumantran, V., "Aspect Ratio Effects in Low Reynolds Number Flow over a Wortmann Airfoil," Virginia Polytechnic Institute and State University, Blacksburg, Va., Rept. VPI-AERO145, Dec. 1984.